

X-ray Absorption Spectroscopic Studies of the Copper(I) Complexes of Crown Ether Appended Bis{(2-pyridyl)ethyl}amines and Their Dioxygen Adducts

Martinus C. Feiters,^{*,†} Robertus J. M. Klein Gebbink,^{†,‡} V. Armando Solé,^{§,||}
Hans-Friedrich Nolting,[§] Kenneth D. Karlin,[⊥] and Roeland J. M. Nolte[†]

Department of Organic Chemistry, NSR Center, University of Nijmegen, Toernooiveld, NL-6525 ED Nijmegen, The Netherlands, EMBL Outstation at DESY, Notkestrasse 85, 22603 Hamburg, Germany, and Department of Chemistry, Johns Hopkins University, Charles & 34th Streets, Baltimore, Maryland 21218

Received January 7, 1999

An X-ray absorption spectroscopic study of the Cu complexes of the bis{(2-pyridyl)ethyl}-appended monoaza crown ether **1**, diaza crown ether **2**, and diphenylglycoluril diaza basket **3** is reported. Following detailed analysis of the spectra of the crystallographically characterized model compound tetrapyridyl Cu(II) bis(nitrate pyridine) (**4**), the contributions of the ring atoms of the coordinating pyridine to the EXAFS were simulated using a multiple-scattering approach and the final parameters obtained by restrained refinement. Oxygenation of the Cu(I) complexes resulted in a large increase of the intensity of the major peak in the phase-corrected Fourier transform. This was interpreted as evidence for a $\mu\text{-}\eta^2\text{:}\eta^2\text{-peroxo}$ coordination mode of the oxygen between the copper ions, which had changed valence from Cu(I) to Cu(II) as judged from the edge position. This oxygen binding mode is reminiscent of that of hemocyanin, but the Cu–Cu distances are significantly shorter in the model than in the enzyme and vary with solvent. The EXAFS of the oxygenated complexes was simulated in a new approach in which, besides the parameters of the pyridine unit, those of an additional multiple scattering unit describing the geometry of the Cu–O₂–Cu moiety were also refined.

Introduction

Hemocyanin, the oxygen transport protein of arthropods and mollusks, has been demonstrated in crystallographic studies to bind molecular oxygen between the two copper ions, which are held in the active site of the protein by two sets of three imidazole ligands.^{1–6} In the past two decades, the details that became gradually known about the coordination chemistry and mode of oxygen binding of hemocyanin and the related enzyme tyrosinase have inspired chemists to mimic the structure and function of these proteins. Cu complexes of a variety of synthetic ligands, e.g., pyrazoles,^{7–9} imidazoles,^{10–13} triazacyclononanes,^{14,15}

1,2-cyclohexyl-diamines,^{16,17} and pyridine^{18–21} ligands, have been synthesized and studied in detail.

Next to X-ray diffraction studies on single crystals,^{1–6,8,14,18} X-ray absorption spectroscopy, including extended X-ray absorption fine structure (EXAFS) and X-ray absorption near-edge spectroscopy (XANES), has been the most useful technique to obtain structural information on the deoxygenated and (often unstable) oxygenated complexes of both the biological^{22–27} and the synthetic^{10–12,15,16,28–30} dinuclear copper systems.

* To whom correspondence should be addressed. E-mail mcf@sci.kun.nl. Fax +.31.24.3652929.

† University of Nijmegen.

‡ Present address: Department of Chemistry, Stanford University, Stanford, CA 94305-5080.

§ EMBL Outstation at DESY.

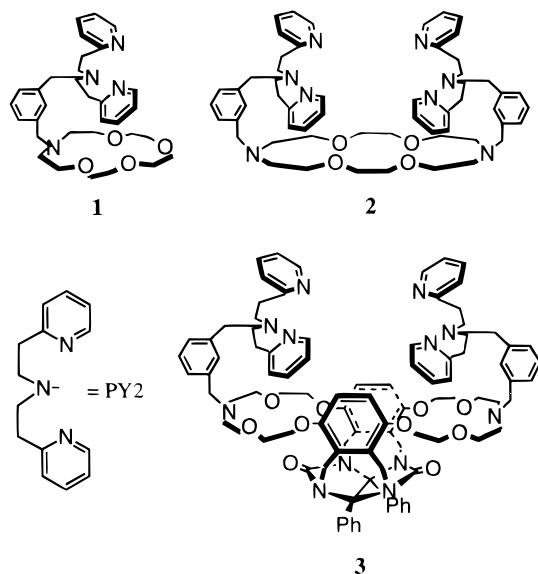
|| Present address: ESRF BP 220, F-38043 Grenoble Cedex, France.

⊥ Johns Hopkins University.

- (1) Magnus, K. A.; Hazes, B.; Ton-That, H.; Bonaventura, C.; Bonaventura, J.; Hol, W. G. J. *Proteins: Struct., Funct., Genet.* **1994**, *19*, 302–309.
- (2) Volbeda, A.; Hol, W. G. J. *J. Mol. Biol.* **1989**, *209*, 249–279.
- (3) Gaykema, W. P. J.; Hol, W. G. J.; Vereijken, J. M.; Soeter, N. M.; Bak, H. J.; Beintema, J. J. *Nature* **1984**, *309*, 23–29.
- (4) Hazes, B.; Magnus, K. A.; Bonaventura, C.; Bonaventura, J.; Dauter, Z.; Kalk, K. H.; Hol, W. G. J. *Protein Sci.* **1993**, *2*, 576–619.
- (5) Magnus, K. A.; Ton-That, H.; Carpenter, J. E. *Chem. Rev.* **1994**, *94*, 727–735.
- (6) Cuff, M. E.; Miller, K. I.; van Holde, K. E.; Hendrickson, W. A. *J. Mol. Biol.* **1998**, *278*, 855–870.
- (7) Sorrell, T. N. *Tetrahedron* **1989**, *45*, 3–69.
- (8) Kitajima, N.; Fujisawa, K.; Moro-oka, Y.; Toriumi, K. *J. Am. Chem. Soc.* **1989**, *111*, 8975–8976.
- (9) Kitajima, N.; Fujisawa, K.; Fujimoto, C.; Muro-oka, Y.; Hashimoto, S.; Kitagawa, T.; Toriumi, K.; Tatsumi, K.; Nakamura, A. *J. Am. Chem. Soc.* **1992**, *114*, 1277–1291.

- (10) Sanyal, I.; Strange, R. W.; Blackburn, N. J.; Karlin, K. D. *J. Am. Chem. Soc.* **1991**, *113*, 4692–4693.
- (11) Sanyal, I.; Karlin, K. D.; Strange, R. W.; Blackburn, N. J. *J. Am. Chem. Soc.* **1993**, *115*, 11259–11270.
- (12) Lynch, W. E.; Kurtz, D. M., Jr.; Wang, S.; Scott, R. A. *J. Am. Chem. Soc.* **1994**, *116*, 11030–11038.
- (13) Sorrell, T. N.; Allen, W. E.; White, P. S. *Inorg. Chem.* **1995**, *34*, 952–960.
- (14) Halfen, J. A.; Mahapatra, S.; Wilkinson, E. C.; Kaderli, S.; Young, V. G., Jr.; Que, L., Jr.; Zuberbühler, A. D.; Tolman, W. B. *Science* **1996**, *271*, 1397–1400.
- (15) Mahapatra, S.; Halfen, J. A.; Wilkinson, E. C.; Pan, G.; Wang, X.; Young, V. G., Jr.; Cramer, C. J.; Que, L., Jr.; Tolman, W. B. *J. Am. Chem. Soc.* **1996**, *118*, 11555–11574.
- (16) DuBois, J.; Mukherjee, P.; Collier, A. M.; Mayer, J. M.; Solomon, E. I.; Hedman, B.; Stack, T. D. P.; Hodgson, K. O. *J. Am. Chem. Soc.* **1997**, *119*, 8578–8579.
- (17) Mahadevan, V.; Hou, Z.; Cole, A. P.; Root, D. E.; Lal, T. K.; Solomon, E. I.; Stack, T. D. P. *J. Am. Chem. Soc.* **1997**, *119*, 11996–11997.
- (18) Jacobson, R. R.; Tyeklár, Z.; Farooq, A.; Karlin, K. D.; Liu, S.; Zubieta, J. *J. Am. Chem. Soc.* **1988**, *110*, 3690–3692.
- (19) Karlin, K. D.; Zuberbühler, A. D. In *Bioinorganic Catalysis*; Reedijk, J., Bouwman, E., Eds.; Marcel Dekker, Inc.: New York, 1999; pp 469–534.
- (20) Karlin, K. D.; Lee, D.-H.; Kaderli, S.; Zuberbühler, A. D. *Chem. Commun.* **1997**, 475–476.
- (21) Karlin, K. D.; Tyeklár, Z.; Farooq, A.; Haka, M. S.; Ghosh, P.; Cruse, R. W.; Gultneh, Y.; Hayes, J. C.; Toscano, P. J.; Zubieta, J. *Inorg. Chem.* **1992**, *31*, 1436–1451.

Chart 1



Having been studied by biologists and bioinorganic chemists for some time, hemocyanins have recently started to attract the attention of researchers working in the field of supramolecular chemistry, as these proteins are among nature's most interesting examples of supramolecular structures, whose assembly, functionality, and cooperativity are controlled by a variety of cations and anions.^{31,32} Inspired by this biological example, we have modeled^{33–36} the cation-induced assembly of relatively inert monomers into a functional assembly by designing and synthesizing a molecule in which a receptor for potassium ions, viz. a crown ether, is covalently linked to a single ligand for Cu(I), viz. bis{(2-pyridyl)ethyl} amine ("PY2"), yielding the "monoaza" compound **1** (Chart 1). The rate of the oxygen

binding by the Cu(I) complex of this ligand system was dramatically increased in the presence of potassium ions, which were proposed to act by binding two crown ether moieties and thereby preorganizing the relatively inert mononuclear Cu(I) complex into a dinuclear Cu(I) assembly of higher oxygen affinity. This study was recently extended³⁶ to the synthesis and multispectroscopic study of the Cu complexes of a "diaz" crown ether **2** and a bisaza "basket" molecule **3** functionalized with 2 ligand sets. Herein, we describe an X-ray absorption spectroscopic study of a number of Cu(I) complexes of ligands **1–3**, in a variety of circumstances (different solvents, presence of oxygen) and of the crystallographically characterized³⁷ model compound tetrapyrridylcopper(II) bis(nitrate pyridine) (**4**).

Experimental Section

The ligands **1–3** and their Cu(I) complexes were synthesized and prepared as described elsewhere.^{35,36} The estimated final Cu concentrations in the samples were around 10 mM. The solid compound **4** was prepared as described before³⁷ and diluted in boron nitride. EXAFS measurements were carried out in the European Molecular Biology Laboratory (EMBL) Outstation in the Hamburg Synchrotron Laboratory (HASYLAB) at the Deutsches Elektronen Synchrotron (DESY) in Hamburg, Germany. The EXAFS station features an order sorting monochromator, which was set to 50% of peak intensity to suppress harmonics, a CANBERRA 13 element solid-state fluorescence detector, and an energy calibration device.³⁸ Typically 4–10 scans/sample were taken. The samples were kept at 20 K in the He exchange gas atmosphere of a closed-cycle cryostat during the measurements and moved in between the scans so that the part of the sample that was exposed to the beam was varied as much as possible. No spectroscopic differences between the scans were observed.

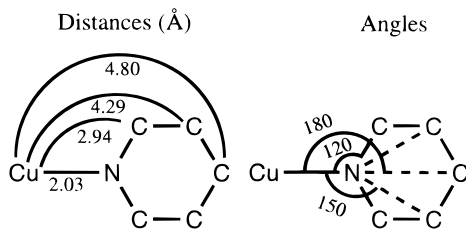
Data reduction was carried out on VAX computers at the Bijvoet Center, University of Utrecht, and the CAOS-CAMM Center, University of Nijmegen, with the EMBL Outstation data reduction package including the energy calibration programmes CALIB and ROTAX, the averaging programme MEAN, and the background subtraction programme EXTRACT. The energy of some of the X-ray fluorescence spectra of our complexes with dichloromethane as the solvent could not be properly calibrated due to the relatively high absorption by this solvent. Simulations of the calibrated, averaged, and background-subtracted EXAFS were carried out on the Daresbury Laboratory (Warrington, U.K.) dedicated X-ray absorption spectroscopy UNIX computer xrsrvl with the programme EXCURV92,^{39–41} including the programme MUFPO for the ab initio calculation of phase shifts and backscattering factors.

For the analysis of the EXAFS we proceeded as follows. First, shells were Fourier filtered and preliminarily analyzed for atom type. In the final simulations, parameter values for the threshold energy value, ΔE_0 , the occupancy of shell i , N_i , the distance to the central Cu absorber of shell i , r_i , and the Debye–Waller-type factor, equivalent to $2\sigma^2$ and describing the thermal and static disorder of shell i , a_i , were entered and adjusted to match the experimental spectrum and subsequently refined by iteration, minimizing the difference between experimental spectrum and simulation as expressed in the fit index. In our simulations of the crystallographically characterized model compound tetrapyrridylcopper(II) bis(nitrate pyridine) (**4**),³⁷ the best agreement between EXAFS and crystal structure was obtained by simulations with phase shifts which were calculated with the EXCURV92 subroutine with both the ground state and exchange values set to X- α . We also noted (see

- (22) Brown, J. M.; Powers, L.; Kincaid, B.; Larrabee, J. A.; Spiro, T. G. *J. Am. Chem. Soc.* **1980**, *102*, 4210–4216.
- (23) Co, M.-S.; Hodgson, K. O. *J. Am. Chem. Soc.* **1981**, *103*, 3200–3201.
- (24) Spiro, T. G.; Woolery, G. L.; Brown, J. M.; Powers, L.; Winkler, M. J.; Solomon, E. I. In *Copper Coordination Chemistry: Biochemical and Inorganic Perspectives*; Karlin, K. D., Zubieta, J., Eds.; Adenine Press: New York 1983; pp 23–41.
- (25) Woolery, G. L.; Powers, L.; Winkler, M. J.; Solomon, E. I.; Spiro, T. G. *J. Am. Chem. Soc.* **1984**, *106*, 86–92.
- (26) Feiters, M. C. *Comments Inorg. Chem.* **1990**, *11*, 131–174.
- (27) Feiters, M. C.; Klein Gebbink, R. J. M.; Martens, C. F.; Nolte, R. J. M.; Karlin, K. D.; Solé, V. A.; Noltling, H.-F.; Hermes, C.; Hazes, B.; Magnus, K. A.; Godette, G.; Bonaventura, C. In *Proceedings of EUROBIIC 3*; Feiters, M. C., Hagen, W. R., Veeger, C., Eds.; NJR Center: Nijmegen, The Netherlands, 1996; F5.
- (28) Karlin, K. D.; Ghosh, P.; Cruse, R. W.; Farooq, A.; Gultneh, Y.; Jacobson, R. R.; Blackburn, N. J.; Strange, R. W.; Zubieta, J. *J. Am. Chem. Soc.* **1988**, *110*, 6769–6780.
- (29) Blackburn, N. J.; Strange, R. W.; Cruse, R. W.; Karlin, K. D. *J. Am. Chem. Soc.* **1987**, *109*, 1235–1237.
- (30) Blackburn, N. J.; Strange, R. W.; Farooq, A.; Haka, M. S.; Karlin, K. D. *J. Am. Chem. Soc.* **1988**, *110*, 4263–4272.
- (31) van Holde, K. E.; Miller, K. I. *Q. Rev. Biophys.* **1982**, *15*, 1–29.
- (32) Ellerton, H. D.; Ellerton, N. F.; Robinson, H. A. *Prog. Biophys. Mol. Biol.* **1983**, *41*, 143–248.
- (33) Martens, C. F.; Klein Gebbink, R. J. M.; Kenis, P. J. A.; Schenning, A. P. H. J.; Feiters, M. C.; Karlin, K. D.; Nolte, R. J. M. In *Bioinorganic Chemistry of Copper*; Karlin, K. D., Tyeklár, Z., Eds.; Chapman & Hall: New York, London, 1993; pp 374–381.
- (34) Klein Gebbink, R. J. M.; Feiters, M. C.; Karlin, K. D.; Nolte, R. J. M. *J. Inorg. Biochem.* **1995**, *59*, 682.
- (35) Klein Gebbink, R. J. M.; Martens, C. F.; Feiters, M. C.; Karlin, K. D.; Nolte, R. J. M. *Chem. Commun.* **1997**, 389–390.
- (36) Klein Gebbink, R. J. M.; Martens, C. F.; Kenis, P. J. A.; Jansen, R. J.; Noltling, H.-F.; Solé, V. A.; Feiters, M. C.; Karlin, K. D.; Nolte, R. J. M. *Inorg. Chem.* **1999**, in press.

- (37) Beurskens, G.; Martens, C. F.; Nolte, R. J. M.; Beurskens, P. T.; Smits, J. M. M. *J. Chem. Crystallogr.* **1995**, *25*, 425–427.
- (38) Hermes, C.; Gilberg, E.; Koch, M. H. J. *Nucl. Instrum. Methods* **1984**, *222*, 207–214.
- (39) Gurman, S. J.; Binsted, N.; Ross, I. *J. Phys. C., Solid State Phys.* **1984**, *17*, 143–151.
- (40) Gurman, S. J.; Binsted, N.; Ross, I. *J. Phys. C., Solid State Phys.* **1986**, *19*, 1845–1861.
- (41) Binsted, N.; Campbell, J. W.; Gurman, S. J.; Stephenson, P. C. EXCURV92, SERC Daresbury Laboratory, 1991.

Scheme 1. Schematic Representation of the Pyridine Coordination in Tetrapyridylcopper(II) Bis(nitrato pyridine), Adapted from Ref 37



Results and Discussion) that multiple-scattering contributions are important throughout the EXAFS region of the spectrum. In the present work, simulations of single shells with single-shell theory were only used to get an impression of the nature and occupancy of the main shells and for preliminary identification of atom types involved in the outer shells. The use of multiple rather than single scattering theory for the simulations has as an additional bonus that the low-energy range (0–25 eV), which has the best signal-to-noise ratio but cannot be simulated adequately with single scattering theory, could be included in the simulation. This enhances the resolution of the Fourier transform and allows better discrimination between the effects of occupancy and Debye–Waller-type factors on the amplitude. In the multiple-scattering simulations, all shells assigned to one unit were given the same occupancy. The value for the amplitude reduction factor (AFAC) that gave optimum agreement for the occupancy of the crystallographically characterized compound was 0.8 for the long energy range (including the 0–25 eV domain) used for multiple-scattering simulations and 0.7 for the shorter range used for single-scattering fits.

After each iterative refinement of a simulation involving multiple-scattering units, the unit was plotted and its geometry inspected. In this way we discovered that iterative refinement of the parameters of the pyridine rings in the multiple-scattering simulations can lead to unrealistic values for the angles and distortion of the rings. This occurred sometimes in the simulations of the model compound **4**, and it was a distinct feature of the simulations for the spectra of the Cu complexes of the PY2 compounds **1–3**. In our final simulations, we therefore adapted the restrained refinement approach, which was introduced earlier for imidazole and polypyrrole systems,⁴² for pyridines. This means that the fit index, which is minimized during the iterative refinement, is artificially increased when deviations from an idealized geometry of the coordinating pyridine ring, as based on the crystal structure of tetrapyridylcopper(II) bis(nitrato pyridine) (**4**),³⁷ occur (Scheme 1). We found it sufficient to restrain the interatomic distances of the pyridine ring and to use a ratio of 1 to 1 for R_{1w} and R_{2w} (which are the weights of the contributions to the fit index due to differences between experimental and simulation and between idealized and refined geometry, respectively) to get physically realistic parameters and geometries as a result of the refinement of ΔE_0 , distances, occupancies, Debye–Waller-type factors, and angles. In addition, we extended the approach for the simulation with 2 multiple-scattering units, viz. one to represent the heteroaromatic rings and one to represent the Cu–O₂–Cu diamond core, which was first applied in our studies of hemocyanin,²⁷ to the analysis of the data of oxygenated complexes presented herein.

Results and Discussion

Simulations of the EXAFS of Tetrapyridylcopper(II) Bis(nitrato pyridine) (4). The crystal structure of tetrapyridylcopper(II) bis(nitrato pyridine) is known,³⁷ and the most important geometric details of the pyridine coordination are presented in Scheme 1. The Cu(II) ion is in a plane with the 4 coordinating pyridine nitrogens at 2.03 Å, and the oxygens of 2 weakly coordinating nitrate counterions occupy the axial positions at 2.42 Å. On the basis of the results of the analysis of the EXAFS

of Cu^{43,44} and Zn⁴⁵ imidazole complexes with weakly coordinating perchlorate, it was not expected that the atoms of the counterion would contribute to the EXAFS. In the crystal structure, there are two noncoordinating pyridines per Cu(II) and the Cu(II) ions are at least 10 Å apart.

In the first stages of the analysis of the EXAFS of **4**, the most important shells were Fourier filtered (Figure 1) and analyzed for atom type (Figure 2, Table 1). In this analysis, “N” (or, for higher shells, “C”) is considered to be representative for a group of atoms, whose backscattering power and envelope are difficult to distinguish from each other, viz. the so-called “low-Z” atoms C, N, and O, while S represents a group of second row atoms (P, S, Cl), whose backscattering envelopes are also very similar, but 180° out of phase with the low-Z ligands, and finally, Cu represents the 3d transition metals, which are in phase again with the low-Z ligands but have the maximum in the backscattering envelope shifted to higher k -value. The results showed that the first shell (approximately 2 Å) consists of N-backscattering as expected (Figure 2, left panels). A very good fit could be obtained with N alone at the expected distance and an even better one when the distantly coordinating nitrate oxygen was also included (not shown). For the shell at 3 Å, the results were more ambiguous (Figure 2, middle panels), especially when the ΔE_0 value was allowed to float and to deviate from the value it refined to for the optimum fit for the first shell. Outright misleading results were obtained for the 3rd shell at 4 Å (Figure 2, right panels), where the best match with the backscattering envelope was obtained with Cu, giving a very realistic impression in spite of the nonrealistic occupancy. The apparent good agreement is reminiscent of that found earlier by us in the preliminary analysis of the diaza·Cu(I)₂ compound in dichloromethane, in which a Cu–Cu distance of 4.3 Å was found.³³ This prompted us to investigate the spectra in more detail. As is evident from the crystallographic structure,³⁷ Cu–Cu distances of approximately 4 Å are not realistic for **4**.

We considered that multiple-scattering pathways are important in the X-ray absorption spectra of complexes of pyridine ligands. Initial simulations of EXAFS of model compound **4** confirmed the conclusions of earlier studies on metal complexes with heterocyclic aromatic ligands, viz. imidazoles^{43–46} and pyridines,^{28,30} that multiple-scattering contributions are important over the whole range of the EXAFS of such systems, due to the geometry of the rings where many metal–N(C)–C angles are 180° or close to this value (Scheme 1, right). In fact, we established that Fourier filtering and simulations of backtransformed outer shells by the single-scattering approach, as reported earlier by us,³³ gave unreliable results. This included false positive results for the presence of Cu–Cu contributions where none were expected, for example in the crystallographically characterized model compound **4**.

Multiple-scattering simulations for **4** are shown in Figure 3, and the corresponding parameters are given in Table 2. In all simulations, the distance of the pyridine-N to Cu is less than 0.02 Å below the crystallographic value, which is satisfactory. For the outer shells of the pyridine moiety, the deviation is slightly larger but never more than 0.1 Å. In the case of the

(42) Binsted, N.; Strange, R. W.; Hasnain, S. S. *Biochemistry* **1992**, *31*, 12117–12125.

(43) Strange, R. W.; Blackburn, N. J.; Knowles, P. F.; Hasnain, S. S. *J. Am. Chem. Soc.* **1987**, *109*, 7157–7162.

(44) Strange, R. W.; Hasnain, S. S.; Blackburn, N. J.; Knowles, P. F. *J. Phys.* **1986**, *12-47-C8*, 593–596.

(45) Pettifer, R. F.; Foulis, D. F.; Hermes, C. *J. Phys.* **1986**, *12-47-C8*, 545–550.

(46) Feiters, M. C.; Navaratnam, S.; Al-Hakim, M.; Allen, J. C.; Spek, A. L.; Veldink, G. A.; Vliegthart, J. F. G. *J. Am. Chem. Soc.* **1988**, *110*, 7746–7750.

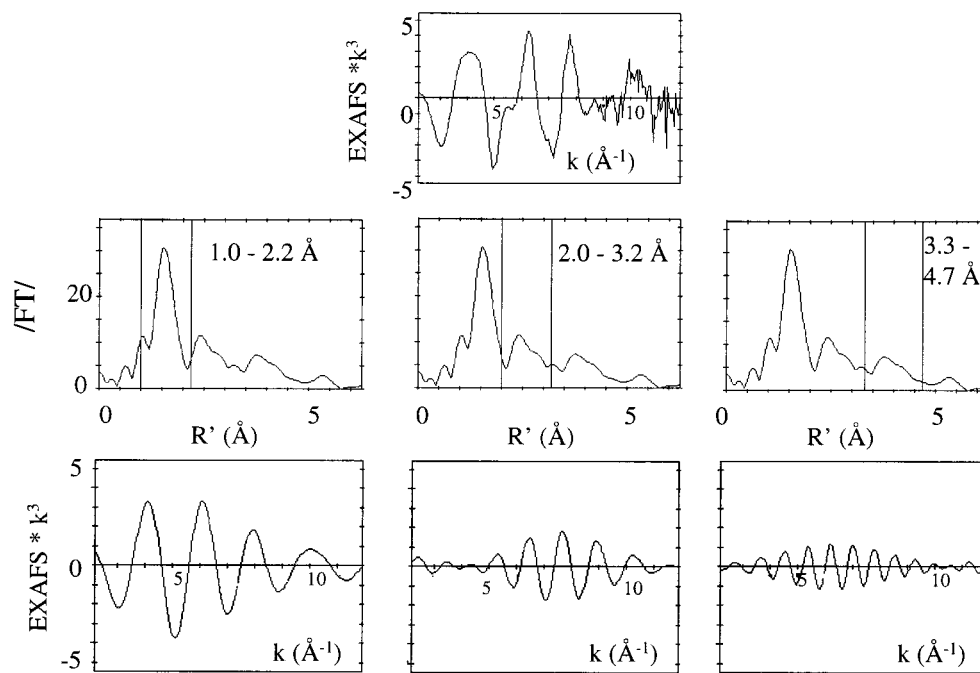


Figure 1. Fourier filtering and back transformation of the EXAFS of tetrapyridylcopper(II) bis(nitrato pyridine) (**4**): top panel, raw EXAFS (k^3 -weighted); middle panels, Fourier transform (non-phase-corrected) with range selected for back transformation, 1.0–2.2 Å (left), 2.0–3.2 Å (middle), and 3.3–4.7 Å (right); bottom panels, back-transformed ranges after the selection in the middle panel had been applied.

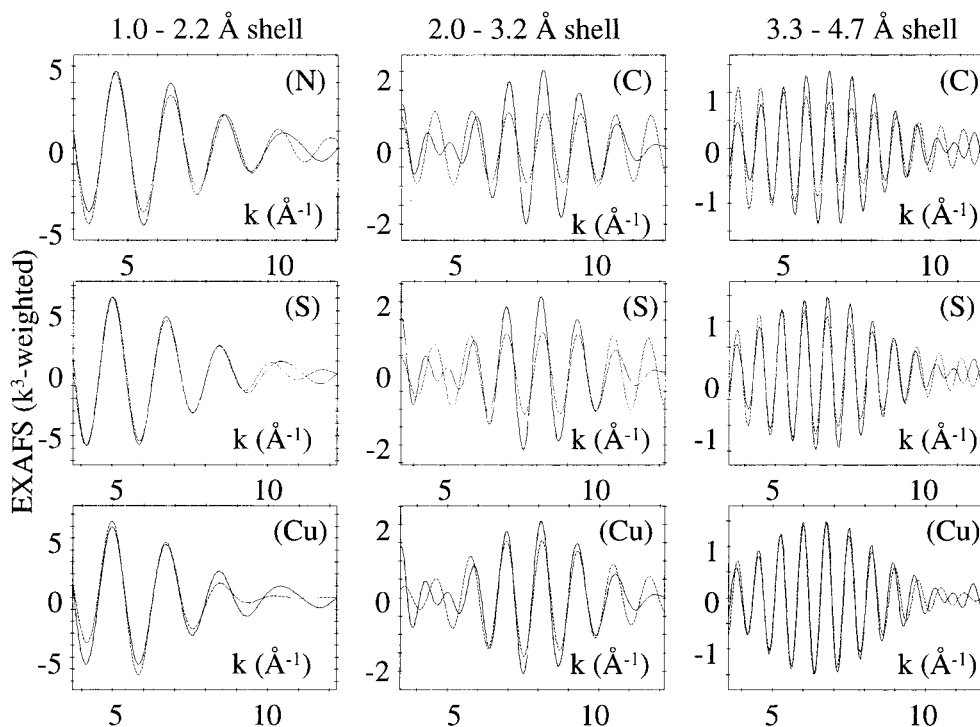


Figure 2. Best fits (parameters in Table 1, dashed lines) for Fourier-filtered and back-transformed shells (solid lines) obtained according to Figure 1. Selection range of Fourier filtering: 1.0–2.2 Å (left); 2.0–3.2 Å (middle); 3.3–4.7 Å (right).

atoms of the nitrate counterion, the distance of the coordinating O to Cu is overestimated (0.1 Å) while a serious disagreement exists for the remote N. For simulation 1 in Table 2 (Figure 3a), the construction of a parameter set based on the crystallographic distances, with Debye–Waller-type factors matched to the intensities of the peaks in the phase-corrected Fourier transform, followed by iterative refinement of ΔE_0 , r , a , N , and the angles in the pyridine unit, resulted in refined values in good agreement with the crystal structure (apart from the nitrate nitrogen occupancy) and reasonable Debye–Waller-type factors.

Because of the lack of restraints for the geometry of the pyridine ring, however, a small distortion occurred (not shown), due to a slight tendency in the multiple-scattering refinement to place C3 and C4 behind C1 and C2, respectively, as seen from the Cu absorber. By introduction of restraints (Figure 3b, simulation 2 of Table 2) on the interatomic distances of the bonds in the pyridine ring, as described earlier for imidazoles and polypyrroles,⁴² this particular distortion was avoided. The fit index was improved, but relatively large spreads in the distance values for C1/C2, and C3/C4, along with the corresponding (slight)

Table 1. Analysis of Single Fourier-Filtered Shells of Tetrapyrildcopper(II) Bis(nitrato pyridine) (**4**), AFAC 0.7 and Energy Range 20–538 eV

	Cu–N or Cu–C				Cu–S				Cu–Cu			
	ΔE_0 (eV)	no.	r (Å)	$2\sigma^2$ (Å ²)	ΔE_0 (eV)	no.	r (Å)	$2\sigma^2$ (Å ²)	ΔE_0 (eV)	no.	r (Å)	$2\sigma^2$ (Å ²)
1st shell (1.0–2.2 Å)	17.0	4.1 @	(N) 2.03	0.016	32.2	4.4 @	2.16	0.028	30.1	15.6 @	1.90	0.065
2nd shell (2.0–3.2 Å)	18.5	1.6 @	(C) 2.90	0.000	27.6	0.6 @	2.99	0.001	24.3	1.2 @	2.87	0.017
3rd shell (3.3–4.7 Å)	18.4	5.2 @	(C) 4.44	0.010	25.2	3.1 @	4.53	0.017	26.9	8.6 @	4.36	0.041

Table 2. Parameters for Simulations of Tetrapyrildcopper(II) Bis(nitrato pyridine) (**4**), AFAC 0.8^a

	cryst struct (av) (Scheme 1)	simulation 1 multiple scattering (Figure 3a)	simulation 2 multiple scattering, restrained refinement, including NO ₃ ⁻ (Figure 3b)	simulation 3 multiple scattering, restrained refinement (Figure 3c)	simulation 4 multiple scattering, nitrate oxygen only (Figure 3d)
range		3.00–545.00	3.00–545.00	3.00–545.00	3.00–545.00
ΔE_0		18.16	19.32	18.61	18.28
pyr-N	4 @	3.9 @	4.2 @	3.4 @	3.5 @
		2.03	2.028 (0.016)	2.017 (0.019)	2.028 (0.015)
pyr-Cl,C2	2.94	2.894 (0.025)	2.941 (0.027)	2.915 (0.027)	2.892 (0.023)
	2.94	2.894 (0.024)	2.854 (0.021)	2.913 (0.028)	2.892 (0.023)
pyr-C3,C4	4.29	4.281 (0.060)	4.276 (0.033)	4.258 (0.061)	4.276 (0.049)
	4.29	4.280 (0.060)	4.132 (0.096)	4.262 (0.056)	4.275 (0.049)
pyr-C5	4.80	4.769 (0.029)	4.732 (0.033)	4.752 (0.026)	4.751 (0.031)
nitrate O	2 @ 2.42	1.6 @ 2.527 (0.022)	1.8 @ 2.514 (0.017)		1.6 @ 2.507 (0.031)
nitrate N	2 @ 3.48	0.7 @ 3.451 (0.027)	1.8 @ 3.210 (0.016)		
fit index		0.000 72	0.000 53	0.000 87	0.000 79

^a Distances in Å; Debye–Waller-type factors as $2\sigma^2$ in parentheses in Å².

asymmetric distortion of the pyridine ring, were found. Reasonable agreement resulted for the distance and occupancy of the nonrestrained nitrate atoms, apart from a large deviation in the distance for the noncoordinating nitrogen. Omission of the nitrate (Figure 3c, simulation 3 of Table 2) resulted in a far higher fit index but a good agreement with the crystal structure and a slight distortion similar to that for simulation 1. The coordination number for the pyridine unit is now closer to 3 than 4. The significant difference in fit index convinces us that the contribution of the nitrate to the spectrum is real, in spite of the weak coordination and the poor agreement for the nitrate parameters with the crystallographic values. Inclusion of the nitrate oxygen alone (and omission of the nitrate nitrogen) also resulted in a significant decrease of the fit index compared to the simulation with only pyridines (Figure 3d, simulation 4 of Table 2). The result that the counterion contributes to the EXAFS is contrary to the results for analogous situations with imidazole perchlorate complexes^{43–45} but in line with recent results for copper complexes with triflate,⁴⁷ BF₄⁻,⁴⁸ and methoxide⁴⁸ counterions.

The conclusions from the study of **4** are that (i) multiple-scattering effects are important in the whole range of the EXAFS, (ii) attempts to analyze the spectra by Fourier filtering and single-scattering simulations give misleading results, including false-positive indentifications of Cu–Cu distances, and (iii) the counterion atoms are found to contribute significantly to the EXAFS.

Cu(I) Complexes of the PY2-Appended Crown Ethers 1–3. The XANES, k^3 -weighted EXAFS, and corresponding Fourier transforms of the Cu(I) complexes of **1–3** in acetonitrile are presented in Figure 4; spectra showing the effect of oxygen on **2**·2Cu(I) in acetone and tetrahydrofuran (THF) are given in

Figure 5. The positions of the edges (top panels of Figures 4 and 5) confirm that the valence state of the copper in all deoxygenated samples is Cu(I). In the edge spectra of the diaza Cu(I) complexes in acetone or THF (or dichloromethane, not shown) a pronounced shoulder is observed (Figure 5, top panel). This shoulder has been ascribed to $1s \rightarrow 4p$ transitions which are lower in intensity when the $4p_x$, $4p_y$, and $4p_z$ levels become degenerate as the symmetry of the coordination geometry increases.⁴⁹ Therefore, the blurring that is observed in the spectra recorded with acetonitrile as the solvent (Figure 4) could point to a different coordination mode in this solvent, involving a solvent molecule. This is not entirely unlikely because four-coordinate copper(I) complexes with PY2 tridentate ligands, plus ligated acetonitrile, CO, or triphenylphosphine, have been reported.²¹ Interestingly, the EXAFS of **1**·Cu(I) in acetonitrile in the presence of excess potassium thiocyanate (not shown) showed that the thiocyanate anion can displace the coordinating solvent molecule on Cu(I) while the nitrogens of **1** are retained as ligands. The amplitudes of the normalized edge spectra at 8984 eV also indicate a change in the coordination of Cu(I) in the complex with **2** going from acetone or THF to acetonitrile; the values for acetone (0.57) and THF (0.56) are in line with 3-coordination (0.54),⁴⁹ while that for acetonitrile (0.36) is much lower than that quoted for 4-coordinated Cu(I) (0.49),⁴⁹ indicating an increase in coordination number as well as a loss of symmetry in the coordination geometry. None of our edge spectra are exactly the same as any of the literature spectra.⁴⁹ The edges of the Cu(I) complexes of **1–3** in acetonitrile have no match whereas those of **2**·2Cu(I) in acetone or THF (or dichloromethane) resemble most that of Cu(TEPA)BPh₄ (TEPA = tris{(2-pyridyl)ethyl}amine).⁵⁰ This compound contains copper in a coordination sphere of 4 nitrogens in an approximately tetragonal geometry, but in view of the amplitude of the normalized edge spectrum (see above), our present EXAFS results (see

(47) Mahadevan, V.; DuBois, J. L.; Hedman, B.; Hodgson, K. O.; Stack, T. D. P. *J. Am. Chem. Soc.* **1999**, *121*, 5583–5584.

(48) Wang, Y.; DuBois, J. L.; Hedman, B.; Hodgson, K. O.; Stack, T. D. P. *Science* **1998**, *279*, 537–540.

(49) Kau, L.-S.; Spira-Solomon, D. J.; Penner-Hahn, J. E.; Hodgson, K. O.; Solomon, E. I. *J. Am. Chem. Soc.* **1987**, *109*, 6433–6442.

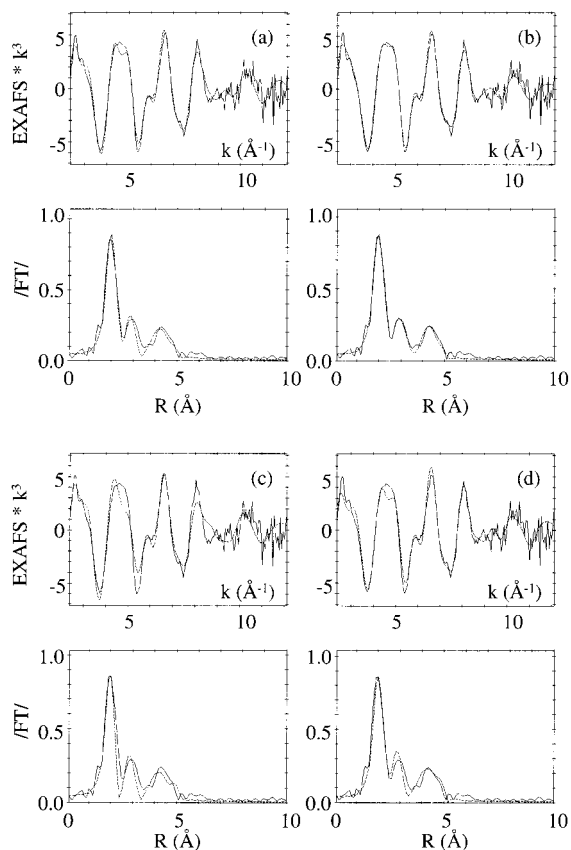


Figure 3. (a) Refined simulations with multiple scattering for the EXAFS (top panel) and Fourier transform (bottom panel) of tetrapyrrolylcopper(II) bis(nitrato pyridine), with parameters given in Table 2. (b) Pyridine units with restrained refinement and atoms of the nitrate counterion included. (c) Pyridine units with restrained refinement. (d) As (b), with only nitrate oxygen. Key: experiments, solid lines; simulations, dashed lines.

below), and previous studies on PY2 systems,^{28–30} we think that 3-coordination is more likely for the Cu(I) complex of **2** in acetone and THF.

Analysis of the Fourier-filtered main shells (Table 3) pointed to coordination by 3 nitrogen (or other low-Z) ligands for the Cu(I) complexes of **1–3**. The fact that the occupancy in acetonitrile was systematically higher than that in acetone (Table 3; see below) may be taken as another weak indication that there is additional coordination by one solvent molecule in acetonitrile. Simulations of the raw (non-Fourier filtered) data with multiple-scattering contributions for the pyridine rings (Figure 6, Table 4) gave optimum agreement with 2 pyridine rings and 1 amine nitrogen, confirming the proposed coordination sphere for Cu. It is of interest to compare the EXAFS and corresponding Fourier transforms (Figure 4, lower panels) of the Cu(I) complexes of **1–3** to see if any evidence for preorganization of the Cu(I) ions can be found. In our preliminary account of the analysis of the EXAFS of 2·2Cu(I) in dichloromethane we proposed, on the basis of the identification of an isolated shell at approximately 4 Å in the Fourier transform, that the copper ions in this complex are preorganized for binding of dioxygen. This would imply that the substituents at the aza atoms in the crown ether are on the same side of the molecule, resulting in a Cu–Cu distance of 4.3 Å. Inspection of spatial models of 2·2Cu(I), however, indicated that such a copper–copper distance is difficult to rationalize; in particular,

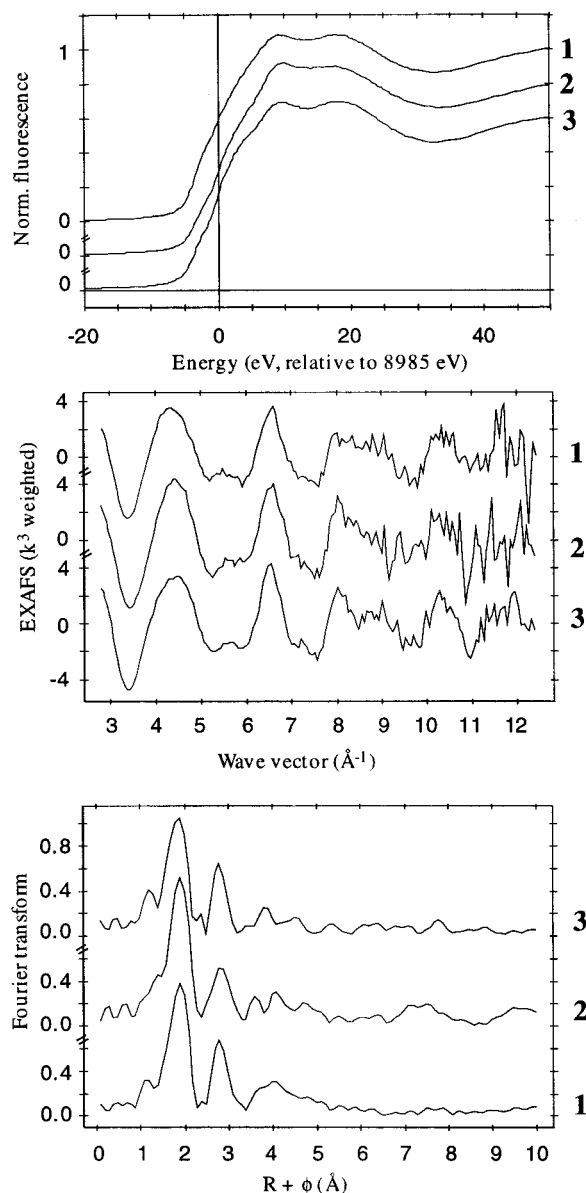


Figure 4. XANES spectra (top), k^3 -weighted EXAFS (middle), and corresponding Fourier transforms (bottom) of the Cu(I) complexes of the PY2-appended monoaza **1**, diaza **2**, and basket **3** in acetonitrile.

its observation in EXAFS, which would require the presence of bridging ligands of some kind, dampening the noncorrelated thermal motion of the coppers, is unlikely. With the results of the present more detailed analysis including simulation of the contributions of the pyridine ring by multiple scattering in hand (Table 4, Figure 6), we find that the whole spectrum can be satisfactorily fitted without an additional Cu–Cu contribution. For all the spectra of the Cu(I) complexes, attempts were made to improve the agreement between experiment and simulation by including such a contribution in the simulation in addition to that of the pyridine rings. The Cu–Cu distance came either in the 3.6–3.8 or the 4.1–4.3 region, but in none of the cases was the decrease in fit index⁵¹ sufficient to justify its inclusion as an additional shell.

Oxygenated Cu(I) Complexes of the PY2-Appended Diaza-Crown Ether 2. Considerable changes in edge, EXAFS, and Fourier transform were observed upon oxygenation of the

(50) Karlin, K. D.; Hayes, J. C.; Hutchinson, J. P.; Hyde, J. R.; Zubieta, J. *Inorg. Chim. Acta* **1982**, *64*, L219–L220.

(51) Joyner, R. W.; Martin, K. J.; Meehan, P. *J. Phys. C., Solid State Phys.* **1987**, *20*, 4005–4012.

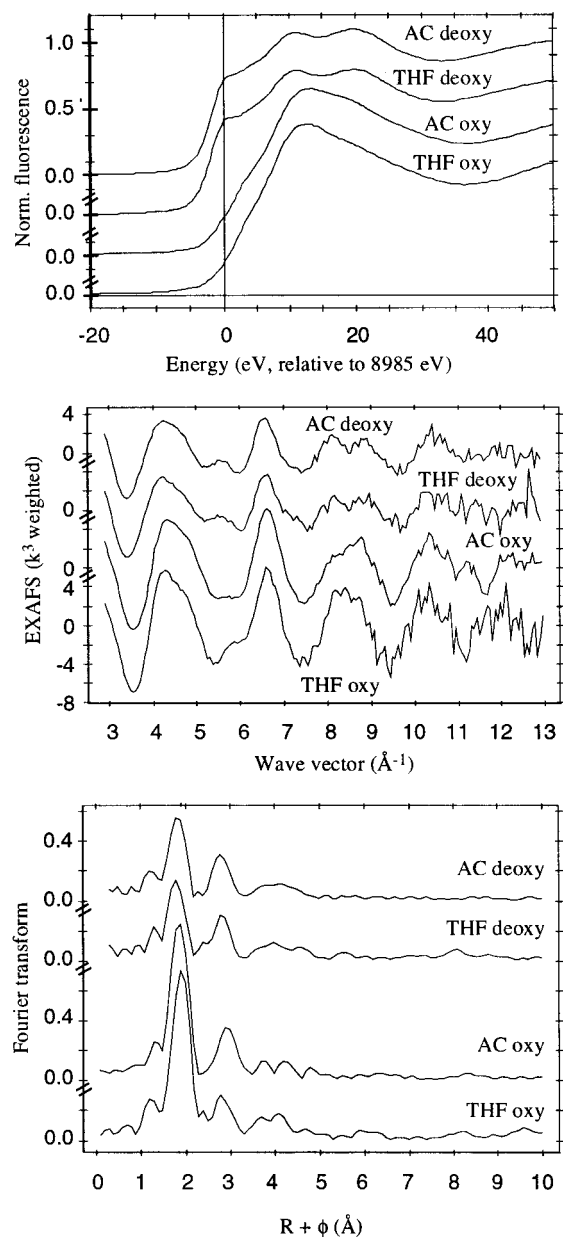


Figure 5. XANES spectra (top), k^3 -weighted EXAFS (middle), and corresponding Fourier transforms (bottom) of the PY2-appended diaza **2** in, from top to bottom, acetone under Ar, acetone with O₂, THF under Ar, and THF under O₂.

2·2Cu(I) complex (Figure 5). The effect on the edge is similar to that observed upon oxygenation of the oxygen transport protein hemocyanin⁵² and is strong evidence for a change in valence from Cu(I) to Cu(II).⁴⁹ The literature edge spectrum⁴⁹ most similar to that of our oxy complexes is the one reported for the bis Cu(II) monoazide diperchlorato complex of the condensation product of 2-hydroxy-1,3-diaminopropanetetraacetic acid with 1,2-diaminobenzene (4 equiv) followed by N-alkylation with bromoethane (4 equiv). This complex has 4 N ligands and 1 O in an approximately tetragonal-pyramidal stereochemistry around copper.⁵³ It is important to note that the edge spectra of oxygenated **2**·2Cu(I) gave no evidence for the formation of high-valent Cu ions, i.e. Cu(III). Evidence for the

occurrence of Cu(III), in a dinuclear bis(μ -oxo) Cu complex, was found in the X-ray absorption edge of oxygenated cyclohexyldiamine complexes,¹⁶ and the formation of Cu(III) was also implied by crystallographic studies of triazacyclononane and cyclohexyldiamine copper bis(μ -oxo) complexes.^{14,17} Our data pointed to the absence of a dinuclear bis(μ -oxo)copper complex, which is in line with the conclusion from recent resonance Raman studies that such complexes do not generally play a role in the binding and activation of oxygen by PY2-Cu complexes,^{54–56} although an exception has been noted recently.⁵⁷

In the Fourier transform, an approximate doubling in the intensity of the main shell of low-Z atoms at approximately 2 Å was noted upon oxygenation in both acetone and THF, similar to the effect observed for hemocyanin.²⁶ This allows the conclusion that each Cu in the dinuclear complex must coordinate both oxygen atoms of the bound molecular oxygen, corroborating our proposal³⁵ that the oxygen is coordinated in the μ - η^2 : η^2 mode. Single-scattering analysis of the Fourier-filtered main shell showed an increase from an occupancy of 3 for the Cu(I) complex to an occupancy of 4 for the Cu(II) oxy complex (Table 3). We note that this is, within the experimental error typically quoted for determination of the coordination number by EXAFS (20%),⁵⁸ the same as the expected coordination number of 5 and that the appearance of the edge is consistent with 5-coordination. The results of detailed simulations of the full EXAFS including multiple-scattering contributions for the pyridine and Cu–O₂–Cu units also pointed to a coordination by 2 pyridines, 1 (amine) nitrogen, and 2 oxygen atoms per copper (Figure 7a,c, Table 5).

There is a subtle but significant effect of the solvent (THF or acetone, Figure 7b,d) on the oxy spectra, in particular in the region around 3 Å in the Fourier transform and 4 Å⁻¹ in the EXAFS. Recent studies on the copper complexes of 1,4,7-triazacyclononanes¹⁴ have indicated that the exact geometry of the Cu–O₂–Cu moiety, including the Cu–Cu distance and the extent to which the O–O bond is broken, depends on the solvent and on the substituents on the cyclononane. In the EXAFS studies of the cyclononane Cu complexes¹⁵ the assignment of peaks in the Fourier transform to Cu appears to be without any problem. In biological and biomimetic systems and models involving heterocyclic aromatic ligands (imidazole, pyridine) it may be a problem to distinguish Cu from low-Z contributions at the same distance, as such contributions are different only in the envelope of the backscattering amplitude, while the phase relationship between EXAFS and Fourier transform is the same. Scott and co-workers⁵⁹ were pessimistic about the possibility to discriminate between Cu and C with EXAFS using single scattering only, which is in agreement with our present single-scattering results, mentioned above, on the tetrapyrroline Cu model compound **4**. In a more recent study on tris(imidazole) phosphine Cu complexes, using multiple scattering,¹² they are more positive, establishing a Cu–Cu distance of 3.48 Å.

(54) Pidcock, E.; Obias, H. V.; Zhang, C. X.; Karlin, K. D.; Solomon, E. I. *J. Am. Chem. Soc.* **1998**, *120*, 7841–7847.

(55) Obias, H. V.; Lin, Y.; Murthy, N. N.; Pidcock, E.; Solomon, E. I.; Ralle, M.; Blackburn, N. J.; Neuhold, Y.-M.; Zuberbühler, A. D.; Karlin, K. D. *J. Am. Chem. Soc.* **1998**, *120*, 12960–12961.

(56) Pidcock, E.; Obias, H. V.; Abe, M.; Liang, H.-C.; Karlin, K. D.; Solomon, E. I. *J. Am. Chem. Soc.* **1999**, *121*, 1299–1308.

(57) Pidcock, E.; DeBeer, S.; Obias, H. V.; Hedman, B.; Hodgson, K. O.; Karlin, K. D.; Solomon, E. I. *J. Am. Chem. Soc.* **1999**, *121*, 1870–1878.

(58) Teo, B. K. In *EXAFS Spectroscopy, Techniques and Applications*; Teo, B. K., Joy, D. C., Eds.; Plenum Press: New York, London, 1980.

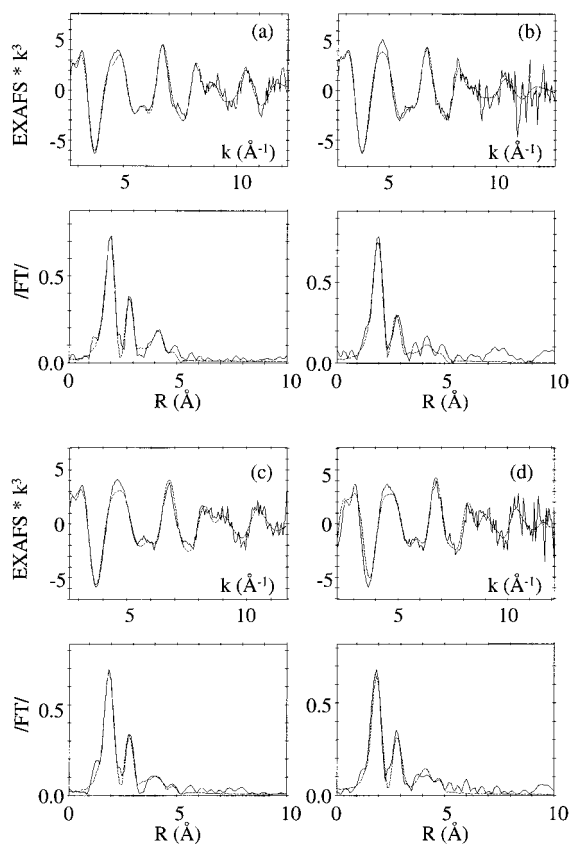
(59) Scott, R. A.; Eidsness, M. K. *Comments Inorg. Chem.* **1988**, *7*, 235–267.

(52) Volbeda, A.; Feiters, M. C.; Vincent, M. G.; Bouwman, E.; Dobson, B.; Kalk, K. H.; Reedijk, J.; Hol, W. G. J. *Eur. J. Biochem.* **1989**, *181*, 669–673.

(53) McKee, V.; Dagdigian, J. V.; Bau, R.; Reed, C. A. *J. Am. Chem. Soc.* **1981**, *103*, 7000–7001.

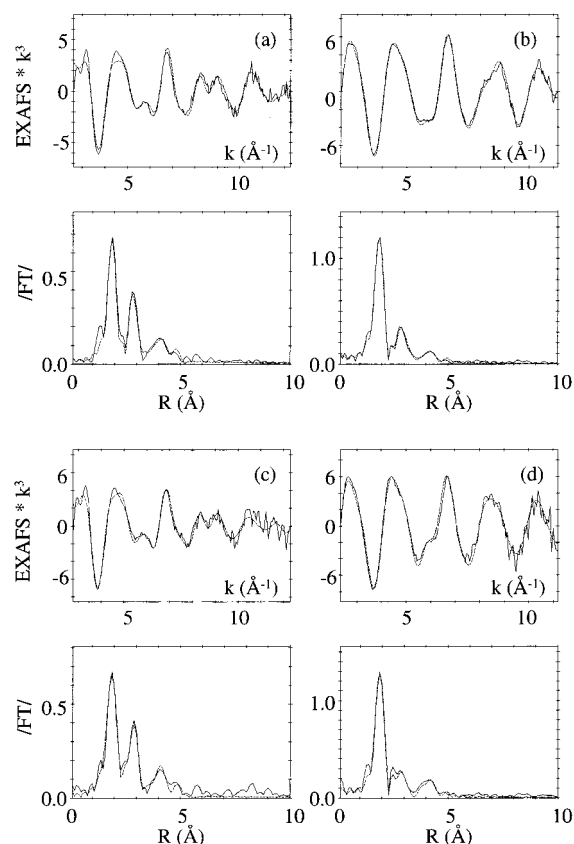
Table 3. Analysis of Main Fourier-Filtered Shells of Cu Complexes of **1–3** with Single-Scattering Theory in Various Circumstances, AFAC 0.7

	Fourier filtering range (Å)	energy range (eV)	ΔE_0 (eV)	Cu–N		
				no.	r (Å)	$2\sigma^2$ (Å ²)
1•Cu(I), acetonitrile	0.9–1.9	19–491	26.85	3.2	1.95	0.016
2•Cu(I), CH ₂ Cl ₂	0.9–2.0	18–550	21.26	3.3	1.95	0.016
2•Cu(I), acetonitrile	1.0–2.1	18–550	22.64	3.4	1.99	0.014
2•Cu(I), acetone	1.0–2.0	18–550	26.93	2.7	1.95	0.012
2•Cu(I), acetone, O ₂	1.0–2.0	19–640	22.68	3.9	1.95	0.009
2•Cu(I), THF	1.0–1.9	18–550	28.31	2.8	1.93	0.015
2•Cu(I), THF, O ₂	1.0–2.2	18–620	21.23	4.0	1.98	0.007
3•Cu(I), acetonitrile	0.9–2.2	18–550	24.65	2.8	1.98	0.015
4, powder in boron nitride	1.0–2.2	20–538	17.10	4.3	2.03	0.016

**Figure 6.** Final simulations, including restrained refinement of the multiple scattering (parameters in Table 4), of the k^3 -weighted EXAFS (top) and corresponding Fourier transform (bottom) of the Cu(I) complexes of (a) PY2- appended basket **3** in acetonitrile, (b) PY2- appended diaza crown ether **2** in acetonitrile, (c) PY2- appended monoaza crown ether **1** in acetonitrile, and (d) **2** in dichloromethane. Key: Experiments, solid lines; simulations, dashed lines.

Blackburn and Karlin³⁰ looked at 3-coordinate Cu pyridine (PY2) complexes related to the ones presented here and found Cu–Cu distances in the range 3.2–3.3 Å by looking at minima in the fit index when the Cu–Cu distance was varied in steps. In their study of the Cu complexes of imidazole ligands,^{10,11} however, they were not able to discriminate between Cu–Cu distances as diverse as 2.84 and 4.30 Å.

In the present study, our approach is similar to that of Blackburn,³⁰ viz. variation of the Cu–Cu distance in steps. We considered, however, that variations in the Cu–Cu distance while the Cu–O (and O–O) distances are kept constant must be accompanied by changes in the angles in the Cu–O₂–Cu diamond core (Figure 8). Having established that multiple scattering is important for the Cu–O₂–Cu diamond core, we also entered the appropriate value for the dihedral angle between the planes through the two Cu–O₂ parts as well as the Cu–

**Figure 7.** Final simulations, including restrained refinement of the multiple scattering of the pyridine unit as well as (where applicable) Cu–O₂–Cu unit (parameters in Table 5), of the k^3 -weighted EXAFS (top) and corresponding Fourier transform (bottom) of the Cu(I) complexes of PY2- appended diaza crown ether **2** in (a) acetone under Ar, (b) acetone with O₂, (c) THF under Ar, and (d) THF with O₂. Key: Experiments, solid lines; simulations, dashed lines.

O–Cu angle in our simulation. It should be noted (Figure 8) that when the dihedral angle decreases from 180 to 90°, the Cu–O–Cu angle decreases from 137 to 82°, thus reducing the relative importance of multiple scattering and of the exact value of the angle for the simulation. After iterative refinement of the parameters, which included the Cu–Cu distance and Cu–O–Cu angle but not the dihedral angle, we looked at the fit index (see Table 6, Supporting Information) and also at the direction in which the Cu–Cu distance was moving during the refinement. For THF, the variations in fit index were disappointingly small but the Cu–Cu distance had the tendency to move to the closest of 2 values, viz. 2.8 and 3.3, with the best defined minimum at 2.8 Å. In the case of acetone, larger variations in the fit index were observed. Minima were observed at 3.1 and 3.3 Å. Cu–Cu distances set at other distances than 3.1 Å, however, had no tendency to move there in the iterative

Table 4. Parameters for Simulations of the Cu(I) Complexes of PY2-Appended Crown Ethers Monoaza **1**, Diaza **2**, and Basket **3**, AFAC 0.8^a

	basket 3 (Figure 6a), acetonitrile	diaza 2 (Figure 6b), acetonitrile	monoaza 1 (Figure 6c), acetonitrile	diaza 2 (Figure 6f), CH ₂ Cl ₂
range (eV)	2.44–500.00	2.40–597.14	2.37–500.00	2.24–545.00
ΔE_0 (eV)	24.15	23.66	23.84	17.09
pyr-N	2.1 @ 1.947 (0.023)	2.4 @ 1.942 (0.017)	2.3 @ 1.950 (0.011)	1.8 @ 1.941 (0.007)
pyr-C1,C2	2.849 (0.016) 2.907 (0.012)	2.892 (0.023) 2.838 (0.020)	2.891 (0.021) 2.872 (0.018)	2.890 (0.014) 2.892 (0.014)
pyr-C3,C4	4.190 (0.049) 4.280 (0.020)	4.269 (0.072) 4.170 (0.072)	4.267 (0.043) 4.223 (0.057)	4.255 (0.035) 4.258 (0.034)
pyr-C5	4.608 (0.019)	4.627 (0.023)	0.618 (0.027)	4.647 (0.016)
amine-N	1.1 @ 2.000 (0.005)	1.2 @ 2.027 (0.010)	0.8 @ 2.089 (0.011)	0.9 @ 2.077 (0.004)
fit index	0.000 48	0.000 92	0.000 58	0.001 50

^a Distances in Å; Debye–Waller-type factors as $2\sigma^2$ in parentheses in Å².

Table 5. Parameters for Simulations of the Cu(I) Complexes of PY2-Appended Diaza Crown Ether **2** in Acetone and THF, under Ar and with O₂, AFAC 0.8^a

	deoxy in acetone (Figure 7a)	oxy in acetone (Figure 7b)	deoxy in THF (Figure 7c)	oxy in THF (Figure 7d)
range	2.37–550.00	2.17–460.00	2.30–550	2.28–460.00
ΔE_0	22.83	17.50	26.74	18.05
pyr-N	2.2 @ 1.952 (0.008)	2.0 @ 2.070 (0.002)	3.1 @ 1.937 (0.019)	2.1 @ 2.066 (0.002)
pyr-C1,C2	2.891 (0.015) 2.873 (0.018)	2.960 (0.018) 2.923 (0.013)	2.892 (0.009) 2.728 (0.017)	2.938 (0.014) 2.937 (0.012)
pyr-C3,C4	4.271 (0.033) 4.241 (0.048)	4.287 (0.061) 4.231 (0.047)	4.220 (0.011) 4.035 (0.028)	4.239 (0.040) 4.238 (0.039)
pyr-C5	4.622 (0.021)	4.723 (0.038)	4.518 (0.033)	4.710 (0.040)
amine-N	0.8 @ 2.122 (0.011)	1.4 @ 2.272 (0.008)	0.1 @ 2.153 (0.006)	1.1 @ 2.267 (0.006)
O		1.1 @ 1.913 (0.002) 1.1 @ 1.913 (0.002)		1.0 @ 1.929 (0.001) 1.0 @ 1.929 (0.001)
Cu		1.1 @ 3.313 (0.047)		1.0 @ 2.788 (0.022)
fit index	0.000 64	0.000 10	0.000 87	0.000 34

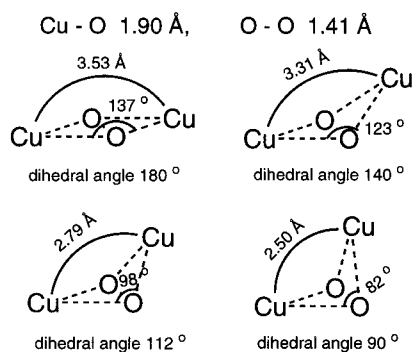


Figure 8. Geometry for the Cu–O₂–Cu unit, with O–O and Cu–O distances derived from the crystal structure of Kitajima:^{8,9} (a) fully extended, with dihedral angle 180°, like in the Kitajima model and in hemocyanin; (b) proposed to exist in diaza–Cu₂–O₂ in acetone on the basis of the present EXAFS analysis; (c) as (b) in THF; (d) extremely bent, dihedral angle 90°.

refinement but moved to 2.85 and 3.3 Å instead. As the simulation with Cu–Cu distances in the region 2.8–2.9 Å did not give minima in the fit index, we suspect that inclusion of Cu at this distance actually leads to “substitution” for pyridine carbon and conclude that the true Cu–Cu distance in acetone is 3.3 Å. The conclusion that the Cu–Cu distances in THF and acetone are 2.8 and 3.3 Å, respectively, is in agreement with the appearance of the intensity of the radial distribution function in the respective Fourier transforms in that region (Figures 5 and 7b,d, bottom).

Concluding Remarks

X-ray absorption spectroscopy is very sensitive to the changes that occur in the ligand geometry of low-valent Cu(I) complexes

upon oxygen binding, and effects of oxygen coordination and concomitant valence changes are readily detected and interpreted. In the study of Cu(I) pyridine complexes, the pitfall of misinterpreting the spectra in terms of Cu–Cu distances can be avoided by a careful treatment of the pyridine rings with multiple-scattering simulations, using restrained refinement techniques to avoid distortions of the ring. The approach described here uses a version of EXCURVE, the earliest EXAFS simulation programme known to describe multiple-scattering effects adequately,⁴³ but other approaches are also valid, viz. those using GNXAS,^{60–65} XFIT,^{66–68} which is based on FEFF 6.01,⁶⁹ or FEFF6.⁷⁰ As these approaches do not appear to offer advantages over those based on EXCURVE, however, a comparison is considered to be outside the scope of the present study. Multiple-scattering contributions are also important in

- (60) Filippini, A.; di Cicco, A.; Natoli, C. R. *Phys. Rev. B* **1995**, *52*, 15122–15134.
 (61) Filippini, A.; di Cicco, A. *Phys. Rev. B* **1995**, *52*, 15135–15149.
 (62) Zhang, H. H.; Filippini, A.; di Cicco, A.; Lee, S. C.; Scott, M. J.; Holm, R. H.; Hedman, B.; Hodgson, K. O. *Inorg. Chem.* **1996**, *35*, 4819–4828.
 (63) Zhang, H. H.; Filippini, A.; di Cicco, A.; Scott, M. J.; Holm, R. H.; Hedman, B.; Hodgson, K. O. *J. Am. Chem. Soc.* **1997**, *119*, 2470–2478.
 (64) Musgrave, K. B.; Angove, H. C.; Burgess, B. K.; Hedman, B.; Hodgson, K. O. *J. Am. Chem. Soc.* **1998**, *120*, 5325–5326.
 (65) D’Angelo, P.; Bottari, E.; Festa, M. R.; Nolting, H.-F.; Pavel, N. V. *J. Phys. Chem. B* **1998**, *102*, 3114–3122.
 (66) Ellis, P. J.; Freeman, H. C. *J. Synchrotron Radiat.* **1995**, *2*, 190–195.
 (67) Rich, A. M.; Armstrong, R. S.; Ellis, P. J.; Freeman, H. C.; Lay, P. A. *Inorg. Chem.* **1998**, *37*, 5743–5753.
 (68) Rich, A. M.; Armstrong, R. S.; Ellis, P. J.; Lay, P. A. *J. Am. Chem. Soc.* **1998**, *120*, 10827–10836.
 (69) Zabinsky, S. I.; Rehr, J. J.; Ankudinov, A.; Albers, R. C.; Eller, M. J. *Phys. Rev. B* **1995**, *52*, 2995–3009.
 (70) Rehr, J. J.; Albers, R. C.; Zabinsky, S. I. *Phys. Rev. Lett.* **1992**, *69*, 3397–3400.

the dinuclear copper site which has oxygen coordinated in the $\mu\text{-}\eta^2\text{:}\eta^2$ mode. We show not only that subtle differences in the geometry of the Cu–O₂–Cu can be detected by X-ray absorption spectroscopy, but also that they can be interpreted. The correlations of our results with other spectroscopic results and reactivity studies have been discussed elsewhere.³⁶ Our spectroscopic results are expected to be important for the studies of both synthetic and biological systems for the binding and activation of molecular oxygen, in view of the omnipresence of both heterocyclic ligand systems^{1–13,18–21} and dinuclear metal sites.^{71,72}

Acknowledgment. The authors thank the Dutch National Science Foundation (SON-NWO, currently CW-NWO) for support and the Northern Atlantic Treaty Organization (NATO) for a travel grant. The European Community is acknowledged for support from their TMR Access to Large Facilities programme, and the CCLRC Daresbury Laboratory, Warrington,

U.K., for computing facilities, including the use of EXCURV92. G. A. Veldink and L. M. van der Heydt (Bijvoet Center, Utrecht, The Netherlands) and W. Jansen (CAOS-CAMM, Nijmegen, The Netherlands) are acknowledged for help with computational facilities, R. de Gelder (Crystallography, Nijmegen) is thanked for help with calculations of radial distribution functions, and H. F. M. Nelissen and H. Engelkamp are acknowledged for preparing the figures.

Supporting Information Available: Table 6, listing starting parameters, final values, and fit indices for the refinement of the simulations of oxygenated 2•2Cu(I). This material is available free of charge via the Internet at <http://pubs.acs.org>.

IC990056Y

(71) Que, L., Jr. In *Proceedings of EUROBIIC 3*; Feiters, M. C., Hagen, W. R., Veeger, C., Eds.; NSR Center: Nijmegen, The Netherlands, 1996; P11.

(72) Que, L., Jr. *J. Chem. Soc., Dalton Trans.* **1997**, 3933–3940.